Controlling the morphology of poly(ethyleneimine)/gold nanoassemblies through the variation of pH and electrolyte additives

Krisztina Bali [a], Mónika Bak [a], Katarina Szarka [b], György Juhász [b], György Sáfrán [c], Béla Pécz [c], Judith Mihály [d], Róbert Mészáros [a,b,*]

[a] Laboratory of Interfaces and Nanosized Systems, Institute of Chemistry, ELTE Eötvös Loránd University, H-1117 Budapest, Pázmány Péter sétány 1/A, Hungary
[b] Department of Chemistry, University J. Selyeho, 945 01 Komárno, Slovakia
[c] Institute of Technical Physics and Materials Sciences, Centre for Energy Research, H.A.S., H-1121 Budapest, Konkoly Thege M. út 29-33, Hungary
[d] Biological Nanochemistry Research Group, Institute of Materials and Environmental Chemistry, Research Centre for Natural Sciences, Hungarian Academy of Sciences, 1117 Budapest, Magyar tudósok körútja 2, Hungary

ARTICLE INFO

ABSTRACT

Recent investigations have revealed very promising analytical and medical applications of poly(ethyleneimine) (PEI) capped gold nanoparticles (Au NPs). One simple way for their synthesis utilizes the dual nature of PEI molecules, which can simultaneously act as reducing and stabilizing agents via their amine groups. However, the formation mechanism of these kinds of NPs as well as the dependence of their morphology and charge on the pH and electrolyte additives has not been explored yet. In the present paper, the role of these factors on the PEI assisted one-pot synthesis of gold nanoassemblies was studied systematically using IR and UV–Vis spectroscopy as well as DLS, electrophoretic mobility and TEM techniques.

It was shown that these nanomaterials cannot be considered as simple PEI coated Au NPs. Instead, the gold particles are embedded in a rather specific polymer matrix, the structure of which ranges from a slightly cross-linked, positively charged thin polymer layer at low pH, to an extended, negatively charged and coherent amorphous polymer film in alkaline medium, provided that adequate type and concentration of supporting electrolyte is also present. These observations were rationalized through the unique pH and salt dependent mechanism of the initial gold(III)/amine complexation and that of the subsequent oxidation and cross-linking processes of the PEI molecules. This crucially determines the following nucleation and growth as well as the morphology, charge and size of the polymer entrapped gold NPs. The presented results may have important implications in novel applications of gold nanoassemblies.

1. Introduction

The importance of gold nanoparticles (Au NPs) in the current nanoscience is incontestable due to their hot potential in a variety of fields such as catalysis, optical, electrical and biomedical devices [1–4]. In nearly all these applications, Au NPs with controlled size, charge and surface properties are needed. Polyelectrolytes are frequently used for the stabilization and further functionalization of Au NPs formed after the reduction of gold(III) ions in aqueous medium. Branched polyethyleneimines (PEI), in particular, are promising candidates for the surface modification of Au NPs due to their dendrimer-like architecture and gene transfection/delivery efficiency [5] as well as their pronounced potential for complexation with oppositely charged entities [6,7].

Recent investigations revealed several analytical applications of PEI capped gold (Au-PEI) NPs including sensing platforms of As(III) [8] and Hg(II) [9] ions as well as the colorimetric detection of heparin [10]. These types of nanosystems have also been proposed as candidates in different biomedical and imaging applications due to their reduced toxicity [11–16]. In addition, interfacial layers of Au-PEI NPs were also utilized recently for surface-enhanced Raman scattering studies [17,18].

The surface conjugation of gold particles with PEI frequently occurs through the interaction of the polyamine molecules with pre-synthetized Au NPs. In these cases, careful removal of the remaining reducing and stabilizing agents is needed. For instance, Cho et al. demonstrated that the remaining amount of citrate ions on the PEI capped gold NPs -prepared from citrate stabilized Au NPs- depends on the PEI addition methods and impacts the properties of the formed polymer conjugated particles [19].

An alternative and much simpler synthetic route utilizes the mild reducing capability of the amine groups of PEI molecules i.e. synthetizing polymer capped Au NPs in the absence of additional reducing agent. A

few one-step synthesis methods of stable PEI capped gold NPs have been reported by several research groups [20–26], which have contributed to the development of new applications [16,18] as well as to the preparation of novel core-shell [27] and inorganic-organic [28,29] nanocomposite materials.

Despite the promising features of the one-pot synthesis, the mechanism of the nucleation and stabilization of polymer capped gold NPs is still not understood. Cho et al. demonstrated that the earlier one pot synthesis studies were controversial and poorly reproducible. The authors revealed in their systematic study that the branched PEI sample of 25 kDa is superior for the preparation of polyamine capped gold particles compared to the linear PEI molecules or to the branched ones with other molar masses. They also showed that the stability and size distribution of the Au-PEI NPs are highly dependent on the ratio of PEI monomers and gold(III) ions [15].

Most of the mentioned investigations are related to mixtures of PEI and HAuCl₄ without any additives and the simultaneous impact of pH and added electrolytes on the formation, charge and morphology of PEI capped gold NPs has not been explored yet. In principle, through the variation of these parameters during the synthetic procedure, the charge, size and structure of the formed Au-PEI nanoassemblies may be tuned in order to make them more efficient and suitable to versatile novel applications. However, for this aim a comprehensive understanding of the combined role of pH, electrolyte type and concentrations in the synthesis of the polymer capped Au NPs is needed.

In this paper, we investigate systematically the PEI assisted synthesis of gold NP assemblies in the presence of different salt concentrations and pH using dynamic light scattering (DLS), electrophoretic mobility, UV–Vis spectroscopy, ATR-IR spectroscopy as well as TEM techniques. It will be shown, that at low and high pH as well as in the presence of different types and concentrations of electrolyte, gold nanoassemblies of remarkably deviating morphology of the embedding polymer matrix can be prepared. We will also demonstrate that these observations are attributable to the pH and salt concentration dependent initial complexation of the gold(III) ions with the amine groups of PEI, which crucially determine their reduction processes, the subsequent nucleation and growth of the Au NPs as well as the morphology of the formed polymer matrix through the oxidation processes of the PEI.

2. Materials and methods

2.1. Materials

The branched poly(ethyleneimine) (PEI, Sigma Aldrich) sample has a mass average molar mass of $M_w = 25$ kDa (from static light scattering) and a number average molar mass of $M_n = 10$ kDa (from GPC) according to the supplier. These PEI molecules contain primary, secondary and tertiary amine groups in an approximate 1:2:1 ratio [30]. HAuCl₄ trihydrate (≥99.9%) was provided by Sigma Aldrich and used as received. NaCl (≥99.5%), NaClO₄ (≥ 98.0%), Na₂CO₃ (≥99.0%), and NaHCO₃ (≥99.7%) were purchased from Merck and used without further purification. Concentrated 70 w/w% HClO₄ (99.99%) solution as well as 1 M HCl (≥99%) and 1 M NaOH (≥98.0%) solutions were the products of VWR. Ultrapure water (Milli-Q) was used for the preparation of the solutions.

2.2. Solution preparation methods

In most of our experiments the effect of different additives on the synthesis of gold nanoparticles was investigated. In these cases, at first the aqueous solution of the additives was mixed with the poly (ethyleneimine) (PEI) solution. Next, the HAuCl₄ solution was added to these mixtures under continuous stirring with a magnetic stirrer (1800 rpm). Then the as-prepared mixtures (10 ml) were heated up and then kept at 80 °C for 2 h. The final PEI (in ethyleneimine (EI) monomer concentration) and HAuCl₄ concentrations were 1.2 mM and 0.2 mM, respectively.

In a couple of cases, the synthesis was carried out in carbonate/bicarbonate buffers. At first, two buffers at the same pH (pH = 10) but with different ionic strengths I (i.e. at two different total concentrations of the carbonate and bicarbonate ions) were prepared, with I = 30 mM and 100 mM, respectively. Next, a concentrated PEI (60 mM in monomer concentration) solution was diluted with the buffer and then 4 mM HAuCl₄ solution was added to this premix under continuous stirring (1800 rpm) to attain the same final composition than for the above-mentioned mixtures (1.2 mM EI monomer and 0.2 mM HAuCl₄ concentrations in 10 ml total volume). The as-prepared mixtures were heated up and then kept at 80 °C for 2 h. The pH of the samples was checked before and after the reaction and it remained constant within experimental error.

2.3. UV–Vis spectroscopy

The formation of Au NPs was monitored by observing changes in the absorption spectra at 25 °C. A Perkin Elmer Lambda 1050 UV/Vis/NIR spectrophotometer was used to record the spectra in the 200–800 nm wavelength interval in a quartz cuvette with path length of 1.00 cm.

2.4. Electrophoretic mobility measurements

The mean electrophoretic mobility (u_ζ) of the Au-PEI NPs was determined at 25.0 ± 0.1 °C, using a Malvern Zetasizer Nano ZSP instrument. The apparatus utilizes the Mixed Measurement Mode - Phase Analysis Light Scattering technique to derive the mean velocity of the particles (v_E) at a given electric field strength (E), from the measured frequency shift of the scattered light due to the moving particles. The mean mobility is determined from the well-known $u_\zeta = v_E/E$ relationship. The values of the electrophoretic mobility were converted to the electrokinetic (or zeta) potential (ζ) of the particles according to the Henry equation [31]:

$$u_\zeta = \frac{\zeta \varepsilon_r \varepsilon_0}{1,5\eta} f(\kappa a) \tag{1}$$

where ε_0 and ε_r are the permittivity of the vacuum and the relative permittivity of the medium, respectively, and η denotes the viscosity of the medium. (Both ε_r and η were approximated with the corresponding values for water at 25 °C). a is the radius of the colloid particle, and κ is the Debye-Hückel parameter ($\kappa = (2000 F^2 c_{el} z^2 / \varepsilon_0 \varepsilon_r RT)^{1/2}$; F is the Faraday number, R is the universal gas constant, T is the absolute temperature, z is the valence of the ions of the symmetrical supporting electrolyte and c_{el} is the electrolyte concentration). $f(\kappa a)$ is a correction factor, which varies between 1.0 and 1.5 for small and large κa values, respectively [31]. It should be noted, however, that the Henry equation is only valid for rigid and compact particles. Therefore, the calculated zeta potential values give only a qualitative indication of the electrokinetic charge of the Au-PEI nanoassemblies at the slipping plane, due to the complex structure of these particles.

2.5. Dynamic light scattering measurements (DLS)

The mean size of the nanoassemblies was monitored by dynamic light scattering. The experimental setup (Brookhaven Instruments) consisted of a BI-200SM goniometer system and a BI-9000 AT digital correlator using a Genesis MX488-1000 OPS laser (1 W). The measurements were carried out at $\lambda = 488$ nm wavelength, at $\theta = 90°$ scattering angle and at 25.0 ± 0.1 °C, 24 h as well as 1 week after the preparation of the systems. The mixtures were filtered through a 0.45 µm pore-size membrane filter prior to the measurements. At first, the normalized electric field autocorrelation functions were analyzed by CONTIN analysis, which revealed wide unimodal distributions of the gold

a.)

b.)
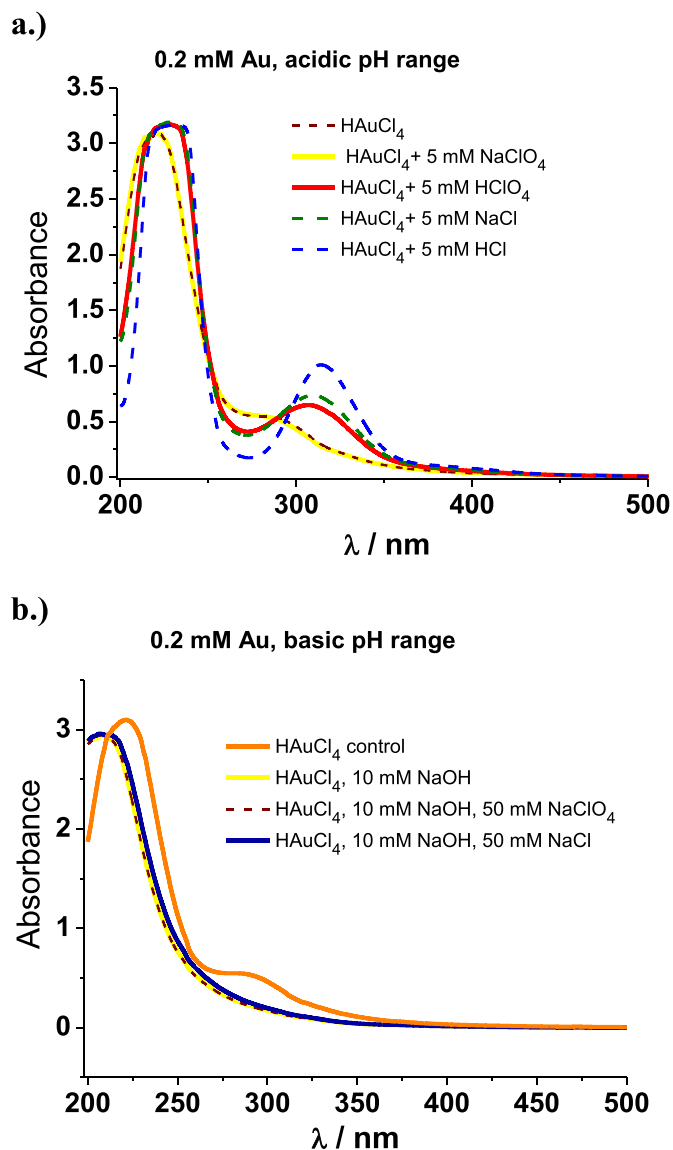
Fig. 1. The UV–Vis spectra of 0.2 mM $HAuCl_4$ solutions in the presence of various additives a.) in acidic and b.) in alkaline medium.
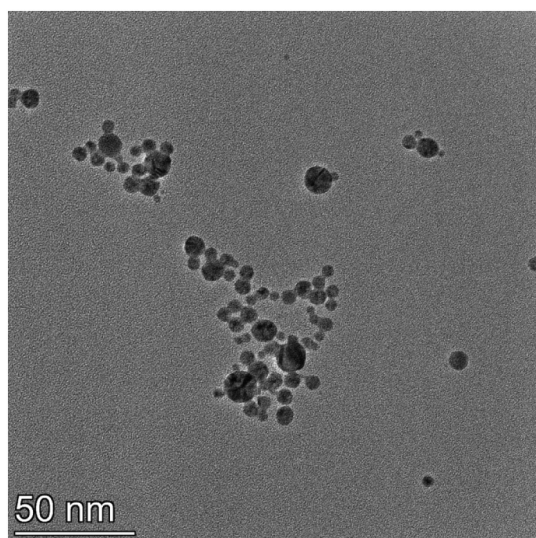
Fig. 2. TEM images of PEI capped gold NPs synthetized in the absence of any additives. c_{Au} = 0.2 mM and c_{PEI} = 1.2 mM, pH = 4.

a.)

b.)

c.)
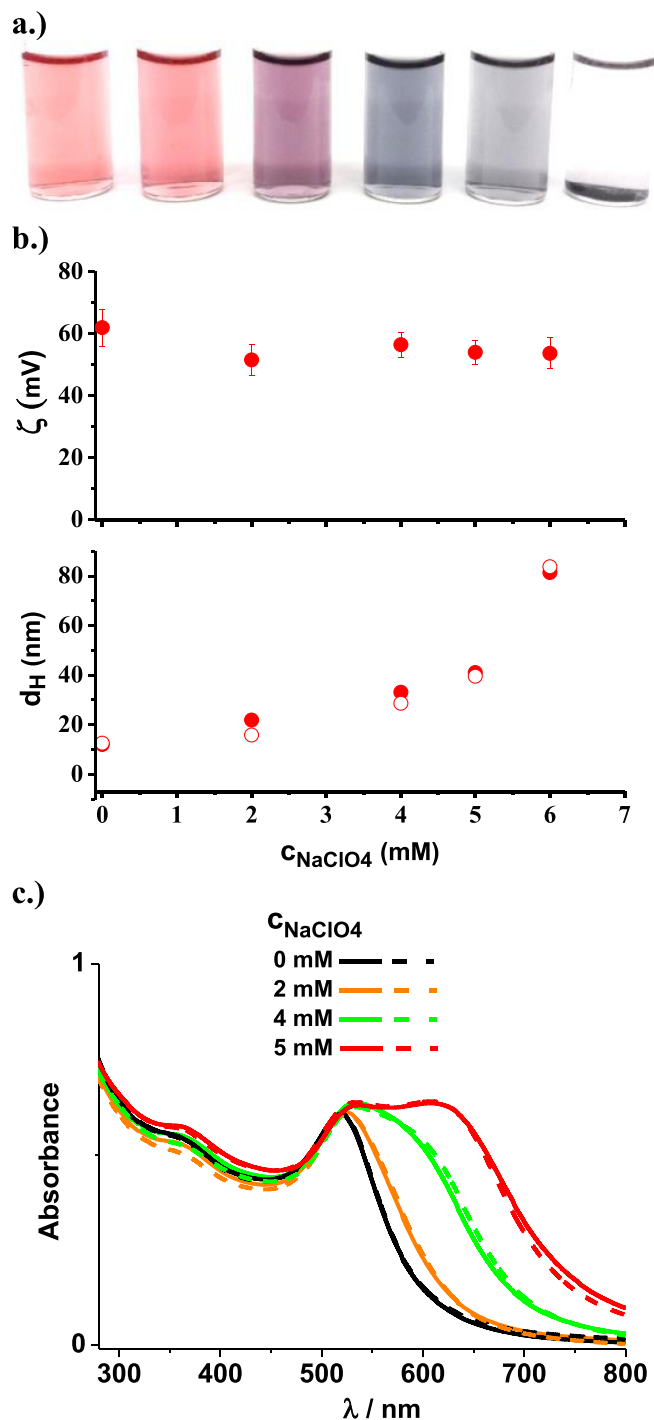
Fig. 3. a.) Photos of gold NP dispersions prepared in the presence of various $NaClO_4$ concentrations (0, 2, 4, 6, 8 and 10 mM). b.) The mean electrokinetic potential and the apparent mean diameter of PEI capped gold NPs as a function of $NaClO_4$ concentration. The solid and open symbols denote the data measured 24 h and 1 week, respectively, after the preparation of the samples. In the case of the DLS data the standard error of the measurements is commensurable with the size of the symbols. (For the sake of clarity, the zeta potential data measured after one week were not plotted since they were equal within experimental error to the values measured 24 h after preparation). c.) The UV–Vis spectra of the dispersions at different $NaClO_4$ concentrations. The solid and dashed lines indicate the spectra measured 24 h and 1 week, respectively, after the preparation of the mixtures. c_{Au} = 0.2 mM and c_{PEI} = 1.2 mM. pH = 4 was found for all these systems (which did not change within experimental error up to one week).
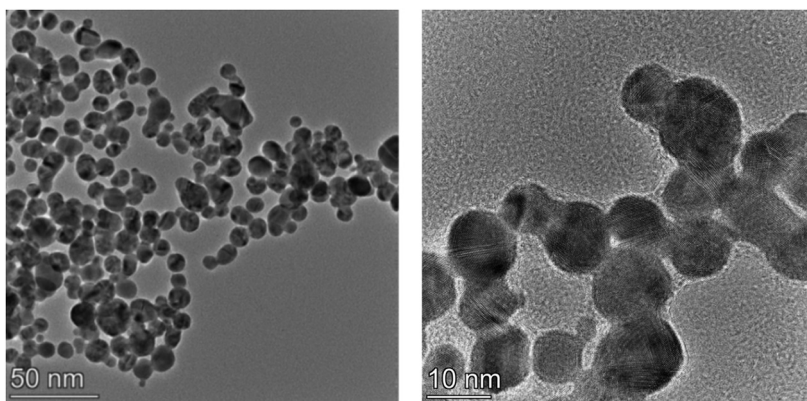
Fig. 4. TEM images of PEI capped gold NPs synthetized in the presence of 5 mM NaClO$_4$. c$_{Au}$ = 0.2 mM and c$_{PEI}$ = 1.2 mM.

nanoassemblies under the applied experimental conditions and compositions. Next, the apparent mean diffusion coefficient of the particles (D_{app}) was derived using the second order cumulant analysis of the autocorrelation functions and their apparent mean hydrodynamic (Stokes) diameter (d_H) was calculated on the basis of the Einstein-Stokes relation assuming spherical particles:

$$D_{app} = \frac{k_B T}{3\pi \eta d_H} \qquad (2)$$

where T is the temperature, k_B is the Boltzmann constant, η is the viscosity of the medium. Occasionally, the apparent mean Stokes diameters were also determined from DLS measurements taken at $\theta = 173°$ scattering angle by the back-scattering utility of the previously described Malvern Zetasizer Nano ZSP instrument using a 10 mW He-Ne laser at $\lambda = 633$ nm. The non-invasive back scattering method slightly attenuates the effect of polydispersity since the measurements at this scattering angle will be less sensitive to the presence of large particles. In the investigated concentration range, the d_H values were not dependent within experimental errors on the type of the applied DLS setups.

2.6. Attenuated total reflection infrared spectroscopy (ATR-IR)

The chemistry of the polymer matrix surrounding the gold nanoparticles was studied by IR spectroscopy. A single reflection diamond ATR unit ('Golden Gate', Specac Ltd., UK) was fitted into a Varian 2000 (Scimitar Series) FTIR spectrometer (Varian Inc., US) equipped with an MCT (Mercury-Cadmium-Telluride) detector. 3 μl of Au-PEI sample was pipetted onto the diamond ATR surface and was gently dried under N$_2$. The formed dry film was measured using 64 scans at a spectral resolution of 2 cm^{-1}.

2.7. Transmission electron microscopy (TEM)

The nanoparticle dispersions were drop-dried on carbon coated microgrids for the TEM study. A Philips CM 20 (200 kV) microscope was used for the conventional electron microscopy (bright field and dark field images) in order to characterize the shape and average diameter of the particles. Particles size was both measured individually on TEM micrographs and tabulated using "ImageJ" a Java-based image processing software. The calculation of the average diameter and its standard error was based on 220–250 particle images. The high-resolution images were taken in a FEI THEMIS 200 image corrected microscope in TEM mode.
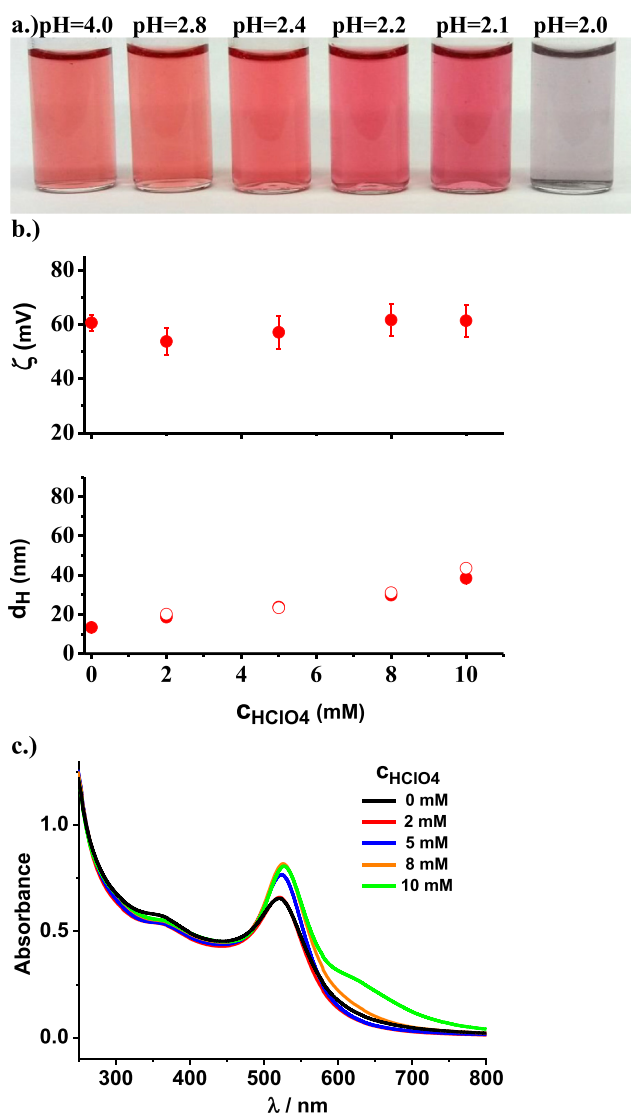
Fig. 5. a.) Photos of gold NP dispersions prepared in the presence of various HClO$_4$ concentrations (0, 2, 4, 6, 8 and 10 mM, with pH = 4, 2.8, 2.4, 2.2, 2.1 to 2, respectively) b.) The mean electrokinetic potential and the apparent mean diameter of PEI capped gold NPs as a function of HClO$_4$ concentration. The solid and open symbols denote the data measured 24 h and 1 week, respectively, after the preparation of the samples. In the case of the DLS data the standard error of the measurements is commensurable with the size of the symbols. (For the sake of clarity, the zeta potential data measured after one week were not plotted since they were equal within experimental error to the values measured 24 h after preparation). c.) The UV–Vis spectra of the dispersions at different HClO$_4$ concentrations measured 24 h after the preparation of the samples. c$_{Au}$ = 0.2 mM and c$_{PEI}$ = 1.2 mM.

3. Results and discussion

3.1. Au-PEI assemblies with positive charges formed at pH ≤ 4

We start our discussion with the properties of gold NP dispersions synthetized at 80 °C from $HAuCl_4$/PEI mixtures in the presence of different $NaClO_4$ or $HClO_4$ concentrations. Under these experimental conditions (pH ≤ 4) positively charged PEI capped gold nanoassemblies are expected to be formed due to the protonated amine groups of PEI remaining after the completion of the reduction process of Au(III) ions [28,29]. The perchlorate ions were preferred to chloride ions due to the involvement of chloride ions in the mixed gold(III)/chloro/hydroxo complex formation [32]. This is clearly demonstrated in Fig. 1, where the UV–Vis spectra of $HAuCl_4$ solutions are shown in the presence of various additives in both acidic and alkaline medium.

As it is indicated by the TEM images in Fig. 2, without any additives (pH ≅ 4), dispersions of quasi spherical, PEI-capped gold NPs are formed with mean diameter values of 7 ± 4 nm by TEM (see the size histogram in Fig. S1) and 12 ± 2 nm by DLS. These results are in agreement with previous studies [28,29] and indicate a significantly wide size distribution of the Au-PEI NPs. This observation is attributed to the polydispersity of the used PEI sample as specified in the experimental part.

In Fig. 3, the photos of the Au-PEI nanosystems, the apparent mean size and the mean electrokinetic potential of the NPs as well as the UV–Vis spectra of their dispersions are shown in the presence of different $NaClO_4$ concentrations. As can be seen, with increasing salt concentration the color of the dispersions changes from rosy to purple and blue, and above 6 mM $NaClO_4$ precipitated systems are formed. In line with this observation, the higher the salt concentration, the larger the apparent mean size of the NPs and the broader the surface plasmon resonance (SPR) peak of the spectra becomes, indicating the appearance of gold NP agglomerates. The electrokinetic potential of the positively charged NPs reveals a shallow minimum and no large reduction of the zeta potential is detectable in the function of $NaClO_4$ concentration. This latter observation is related to the increasing electrokinetic charge of the particles with increasing supporting electrolyte concentration due to the enhanced protonation degree of the amine groups of PEI with increasing ionic strength at the given pH [33].

In Fig. 4, the TEM images of the Au-PEI NPs synthetized in the presence of 5 mM $NaClO_4$ are shown (additional TEM images and the particle size histogram at this composition can be found in Fig. S2). The pictures reveal that – in contrast to the salt free cases – gold aggregates of irregular and asymmetric shapes are formed, which mainly consist of a couple of initially quasi-spherical gold NPs fused into each other during the synthesis process. This is also in line with the lack of a well-

defined SPR peak above 5 mM $NaClO_4$ concentration. Another important observation is that at this composition the mean Stokes diameter of the Au-PEI nanoassemblies from DLS (40 ± 2 nm) is much larger than that of the average TEM diameter of the individual gold NP building blocks (9 ± 3 nm), which also indicates the formation of large agglomerates in the solution phase.

In Fig. 5, the photos of Au-PEI NP dispersions, synthetized in the presence of various $HClO_4$ concentrations as well as the mean electrokinetic potential and the apparent diameter values of the gold nanoassemblies and that of the measured UV–Vis spectra are shown. As can be seen, the increasing amount of $HClO_4$ results in a deepening rosy color and then in the formation of purple precipitates above 10 mM acid concentration. According to Fig. 5b, the zeta potential of the gold nanoassemblies does not change considerably with $HClO_4$ concentration. This also means, that the electrokinetic charge of the Au-PEI NPs increases with the acid concentration due to the increasing protonation degree of the PEI molecules, α_{PEI}, (between pH = 4 and 2, α_{PEI} varies between 0.6 and 0.7 [33]). However, with decreasing pH, the ionic strength of the surrounding medium of the PEI-capped NPs as well as their apparent mean diameter also increases. In contrast to Fig. 3, however, up to 8 mM $HClO_4$ the SPR peak of the UV–Vis spectra remains well-defined and its position is shifted to longer wavelengths suggesting the formation of larger NPs with increasing acid concentration. Characteristic TEM images of PEI capped gold NPs synthetized in the presence of 5 mM $HClO_4$ are shown in Fig. 6. (Additional TEM images and the particle size histogram at this composition are shown in Fig. S3). The pictures reveal quasi-spherical particles, the average TEM diameter (15 ± 6 nm) of which is much larger than that of the primary particles formed at pH = 4. This value is also in reasonable agreement with the apparent mean diameter from DLS (23 ± 2 nm).

These results together suggest that the increasing mean diameter with added $HClO_4$ concentration is primarily the consequence of the formation of larger individual NPs (and not their stable aggregates). The TEM images of Fig. 6 also indicate a thin amorphous interfacial region around the gold particles. This can be clearly seen at the surface of the enlarged particle in Fig. 6. At even higher $HClO_4$ concentrations, i.e. at $c_{HClO_4} \geq 10$ mM, the Au-PEI NPs coagulate during the synthesis and precipitates are formed in agreement with the purple color of the systems and the broadening of their UV–Vis spectra.

3.2. PEI-capped gold NPs synthetized at pH ≥ 10

Since around the neutral pH range (between pH 5.6–8) precipitated systems were formed during the synthesis, we focus our attention on the basic pH range. In Fig. 7, the photos of Au-PEI NP dispersions,
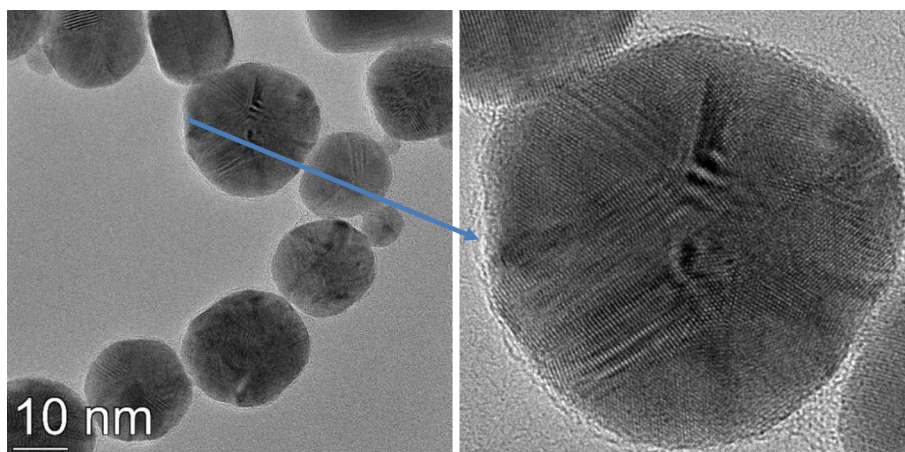
Fig. 6. Left: TEM images of PEI capped gold NPs synthetized in the presence of 5 mM $HClO_4$. Right: An enlarged image of a gold nanoparticle with a thin amorphous shell. $c_{Au} = 0.2$ mM and $c_{PEI} = 1.2$ mM.

K. Bali, M. Bak, K. Szarka et al.

a.)

b.)

c.)
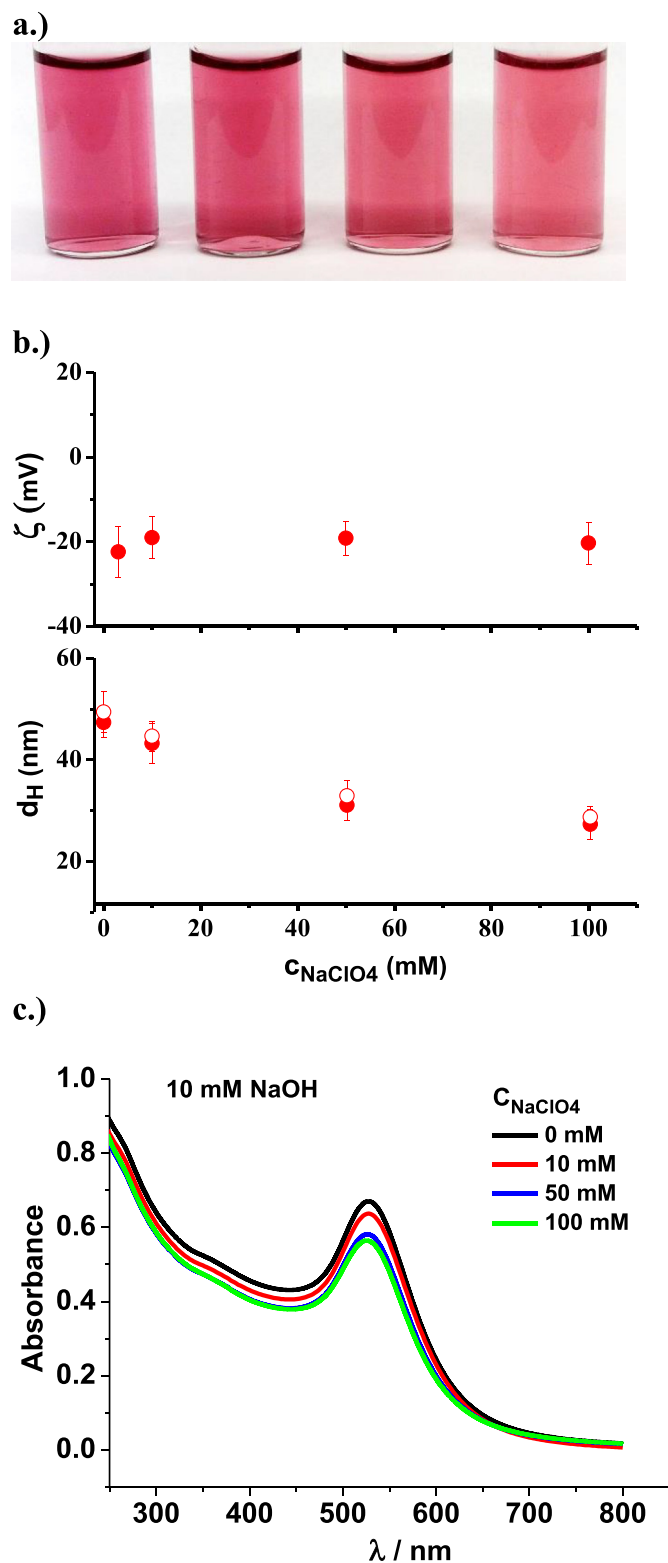
Fig. 7. a.) Photos of gold NP dispersions prepared at different (0, 10, 50, and 100 mM) NaClO$_4$ concentrations in the presence of 10 mM NaOH. pH ≈ 11.5 was found for these nanosystems (which decreased slightly to pH = 11.2 for one week). b.) The electrokinetic potential and the apparent mean diameter of PEI capped gold NPs as a function of NaClO$_4$ concentration. The solid and open symbols denote the data measured 24 h and 1 week after the preparation of the samples, respectively. c.) The UV–Vis spectra of the dispersions at different NaClO$_4$ concentrations. c_{Au} = 0.2 mM and c_{PEI} = 1.2 mM.

synthetized in the presence of 10 mM NaOH with different NaClO$_4$ concentrations (pH ≅ 11.5), are shown together with the mean Stokes diameter and electrokinetic potential of the formed gold nanoassemblies and their corresponding UV–Vis spectra. In sharp contrast with the impact of ionic strength at the acidic pH range, rosy mixtures with reducing color intensity are observable and precipitation does not occur with increasing NaClO$_4$ concentration (up to 100 mM salt concentration). In line with this finding, the mean diameter of the formed Au-PEI nanoassemblies and the absorbance values reduce with increasing electrolyte concentration. An additional remarkable difference compared with Figs. 3 and 5 is the formation of negatively charged gold nanoassemblies (with low zeta potential and electrokinetic charge) in the whole investigated electrolyte concentration range. The observed SPR peaks do not broaden even at large salt concentrations indicating the formation of more regular NPs than at pH 4. This is also revealed in Fig. 8, where the TEM images of Au-PEI NPs synthetized in highly basic medium in the absence and presence of (50 mM) NaClO$_4$ are shown. (Additional TEM images and the particle size histograms at these two compositions are shown in Figs. S4 and S5). An interesting feature of the pictures is that in 50 mM NaClO$_4$, agglomerates of a couple of individual gold NPs are observable, which are embedded in a coherent amorphous film, possibly made of crosslinked PEI molecules. Furthermore, the mean Stokes diameter of the nanoassemblies is much larger than the average TEM diameter of the gold NP building blocks both at low and high ionic strengths (48 ± 4 nm and 28 ± 3 nm from DLS as well as 7 ± 2 nm and 5 ± 2 nm diameter values from TEM analysis, respectively, in the absence and presence of 50 mM NaClO$_4$).

In order to investigate the impact of other types of electrolytes in basic medium, two gold nanosystems were synthetized in bicarbonate/carbonate buffers at the same pH (pH = 10) but with two different ionic strengths; I = 30 and 100 mM, respectively. In both cases, slightly negatively charged Au-PEI nanoassemblies were detected similarly to the data in Fig. 7 (with ζ ≅ −5 and − 10 mV for I = 30 and 100 mM, respectively). The UV–Vis spectra of these systems are shown in Fig. 9. As can be seen, the SPR peak position does not change dramatically, however, the absorbance values are reduced for the buffer with higher ionic strength (similarly to the impact of salt concentration in Fig. 7c). This finding indicates that smaller agglomerates and/or individual gold NPs are formed in the buffer with higher ionic strength (i.e. at larger absolute carbonate/bicarbonate ion concentrations).

The TEM images of the Au-PEI NPs prepared in these buffers are shown in Fig. 10. (The particle size histograms for the buffers with I = 30 and 100 mM are shown in Fig. S6). The pictures reveal that the most regular and smallest gold NPs among all of the investigated systems are observable for the pH 10 buffer with I = 100 mM. However, similarly to the highly basic pH range (Figs. 7 and 8), there is a huge deviation between the apparent mean hydrodynamic diameter of the Au-PEI nanoassemblies and that of the average TEM diameter of their individual gold NPs (22 ± 3 and 12 + 2 nm from DLS as well as 5 ± 2 and 4 ± 2 nm from TEM, for I = 30 and 100 mM ionic strengths, respectively).

3.3. Structural and chemical changes of the PEI molecules in the synthetized Au-PEI NPs

The TEM pictures of the present study indicate the formation of Au-PEI NPs or their agglomerates with different size and shape but with similar polycrystalline internal morphology as several twins and/or fivefold twins observed inside of the individual gold particles [34]. However, the TEM images also reveal that the polymer shell around the Au NPs is largely dependent on the different experimental conditions.

In order to explore qualitatively the variation of the chemistry of PEI molecules in the polymer capped gold NPs, ATR-IR measurements were carried out at the same ratio of PEI and HAuCl$_4$ as previously, but at 10 times higher absolute concentrations of these components (due to sensitivity reasons). In Fig. 11a and b, the ATR-IR spectra of PEI molecules

a.)   b.)
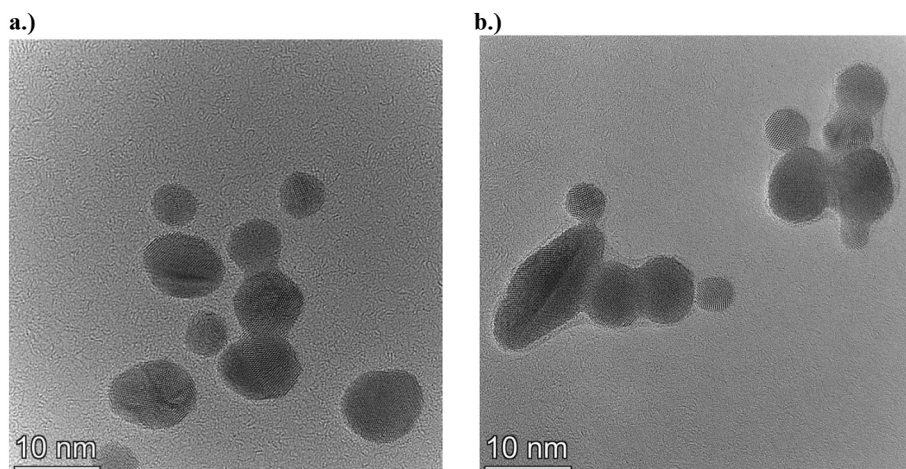
Fig. 8. TEM images of PEI capped gold NPs synthetized in the presence of a.) 10 mM NaOH and b.) 10 mM NaOH and 50 mM $NaClO_4$. $c_{Au} = 0.2$ mM and $c_{PEI} = 1.2$ mM.

and that of the polymer capped gold nanoparticles were compared at pH = 4 and pH = 11, respectively, without added electrolytes.

Pure PEI exhibits the characteristic bands of amine- and ethylene moieties [35,36]. These include the stretching vibration of secondary amines at 3275 cm^{-1} and the antisymmetric and symmetric stretching vibrations of primary amines via the shoulders at 3355 and 3176 cm^{-1} as well as the -NH$_2$ bending bands around 1600 cm^{-1} and the well-defined C—H stretching bands of ethylene groups in the 2920–2800 cm^{-1} wavenumber region. In addition, the band around 1460 cm^{-1} might be a superposition of C—H and N—H bending and the doublet at 1120–1040 cm^{-1} corresponds to the C—N stretching vibrations. Changes in pH, however, cause small but notable changes in the C—H stretching and N—H deformation region. At pH = 4, the C—H stretching region is less defined exhibiting a broad band with peaks at 2955, 2899 and 2839 cm^{-1}. The δN-H band around 1600 cm^{-1} is also split, producing satellite bands at 1507 and 1407 cm^{-1}.

The spectra of polymer capped Au-NPs reveal significant chemical changes in the structure of the PEI molecule after the reduction of

gold(III) ions at both pHs. At pH 4, the CH$_2$ stretching bands are suppressed and a broad band at 3382 cm^{-1} for -NH/-NH$_2$ stretching is dominating the spectra suggesting crosslinking processes in the PEI coating. Furthermore, new bands appear at 1653 and 1612 cm^{-1}, which can be assigned to imine (-CH=N) and enamine vibrations, respectively [35–37]. Occurrence of oxygen-containing functional groups is also suggested by the small carbonyl stretching (νC=O) band at 1744 cm^{-1}. The peculiar frequency of νC=O indicates the presence of aldehyde groups; therefore, it seems plausible that some small aldehyde molecule components are formed during the synthesis procedure.

At pH = 11, the bands corresponding to the stretching of primary and secondary amine groups are similar to the ones measured for pure PEI in highly basic medium. In contrast to the acidic PEI-capped particles, the discrete CH$_2$ stretching bands still exist in the spectrum. However, the νCH$_2$(NH) stretching at 2808 cm^{-1} is largely supressed, which indicate chemical changes due to cross-linking between the different ethyleneimine moieties. The presence of imine groups was witnessed for the Au-PEI NPs prepared at pH = 11, too. In this case the peak position is shifted towards higher wavenumber (to 1665 cm^{-1}), which presumes the formation of further imine groups [35]. No carbonyl band can be detected, and some shoulders appear at 1565 and 1431 cm^{-1}. A possible assignation for these extra bands could be the antisymmetric and symmetric stretching of aminocarboxylates [35].

In the presence of added NaClO$_4$ (Figs. S7 and S8) or carbonate buffer (Fig. S9) the specific contribution of perchlorate and carbonate ions dominate the spectra [35,38]. Nevertheless, similar conclusions can be drawn with respect to the effect of pH on the PEI matrix surrounding the gold NPs. The only difference is observable in the highly basic pH range at 50 mM NaClO$_4$, where the relative ratio of the primary amines of PEI molecules is increased compared to the salt free alkaline medium (see Fig. S7). The summary of the peak assignments related to Fig. 11 and Figs. S7, S8 and S9 can be found in Table S1.

The above-mentioned observations indicate that the chemistry of the polymer matrix in which the gold NPs or agglomerates are embedded considerably differs at low and high pH as well as in the presence of different electrolytes during the synthesis. This result is the consequence of the various pH and electrolyte dependent oxidative dehydrogenation products of the various amine groups during the reduction of gold(III) ions. Upon their oxidation, imine bonds are formed from the ethylene-imine groups with increasing probability at high pH (such as (-NHCH$_2$-CH$_2$-) → (-N=CH-CH$_2$-) + 2H$^+$ + 2 e$^-$) [23,26,39]. Therefore, the formation of -CH=N double bonds is not unexpected, and their presence was also confirmed by independent FTIR and XPS
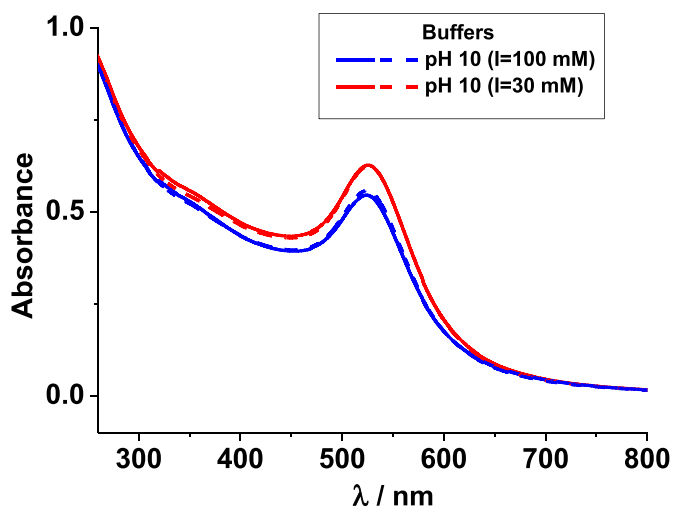
Fig. 9. The UV–Vis spectra of PEI capped gold NP dispersions prepared in carbonate/bicarbonate buffers (pH = 10) at two ionic strengths (I = 30 and 100 mM). The solid and dotted lines denote the spectra measured 24 h and 1 week after the preparation of the samples, respectively. $c_{Au} = 0.2$ mM and $c_{PEI} = 1.2$ mM.

K. Bali, M. Bak, K. Szarka et al.

a.)

b.)

c.)

d.)
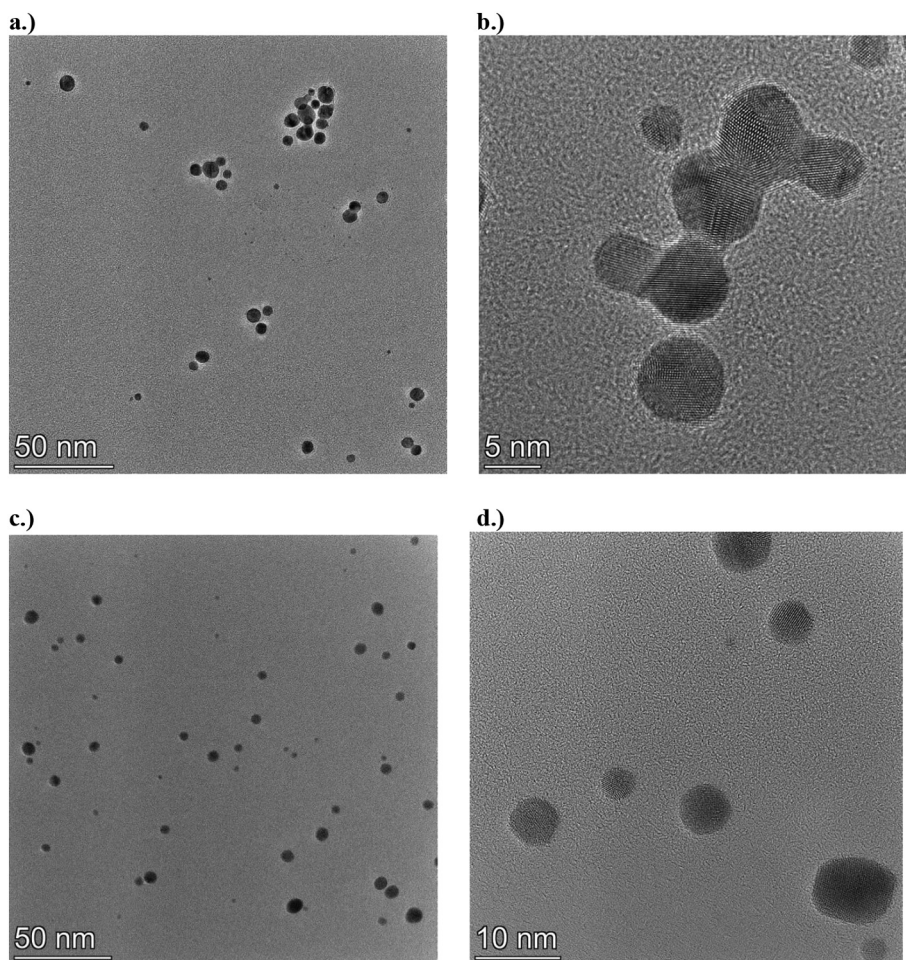
Fig. 10. TEM images of PEI capped gold NPs synthetized in carbonate buffer (pH = 10) a.) and b.) at I = 30 mM as well c.) and d.) at I = 100 mM ionic strengths.

measurements of Kim et al. for PEI capped gold NPs synthetized without additional reducing agent [24]. However, depending on the pH and the applied medium as well as on the chemistry of the amine groups, quite a few alternative oxidation products of alkyl amine groups may also be formed via C—C bond cleavage and/or hydrogen abstraction [40].

3.4. The role of Au^{3+}/PEI complexation in the mechanism of Au-PEI NP formation

One of the key factors, which determine the stability and chemical nature of the formed gold nanoassemblies, is attributable to the initial form of gold(III) ion complexes in the solution. In HAuCl$_4$ solutions, the gold(III) ions are present in the form of Au(III)(Cl$^-$)$_x$(OH)$_y$ complexes with an excess of chloride ions (i.e. x ≅ 2.46 and y ≅ 1.54 at pH 4) [32].

Upon mixing the HAuCl$_4$ solution with PEI at low pH, the negatively charged, mixed chloro/hydroxo complexes of Au^{3+} ions accumulate around the protonated amine groups of the polymer. This promotes the exchange of chloride ions to amine groups around the gold(III) ions, i.e. the conversion into gold(III) amine complexes Au(N-(R-H))$_4^{3+}$, which is also indicated by the sudden appearance of a deep yellow color. This complexation is also indicated in Fig. 12, where the UV–Vis spectra of HAuCl$_4$/PEI mixtures are shown directly after their preparation (i.e. in the absence of gold nanoparticles) in the presence of different additives. The formed Au^{3+}/amine complexes possibly have local planar structures [41].

At pH 4, the primary amine groups of PEI are practically fully and its secondary amine groups are also largely protonated [30], whereas the protonation of the tertiary amine groups is considerably hindered [30,33]. Therefore, at this pH the gold(III)/amine complexes are formed within the core of the PEI molecules with primary involvement of the tertiary and some secondary amine groups. The formation of small aldehyde compounds at low pH is due to the cleavage of the tertiary amine groups as reported for the reduction of gold (III) ions with trimethylamine molecules [42]. This supports the important role of tertiary amine groups in the reduction process in the acidic pH range, which keeps the gold NP core within the PEI molecules.

The formed gold nanoassemblies are stabilized by the charges of the remaining protonated primary and secondary amine groups. Decreasing further the pH by HClO$_4$ addition, there is an optimal pH, where the primary role of the tertiary amine groups is enhanced, and the formed gold NPs are the most stabilized (such as at 5 mM HClO$_4$). On the other hand, in this acidic pH range, C—C cleavage and the formation of reactive carbon radials could also occur [40], which results in a cross-linked PEI matrix around the gold NP core in accordance with the TEM images in Fig. 6. Addition of NaClO$_4$ of increasing concentration during the synthesis at pH 4 leads to asymmetric, large gold nanoassemblies -due to the fusion of the primary particles and the formation of their stable agglomerates- and then to precipitates at the largest applied salt concentrations. With a further decrease of pH, more tertiary amine groups of PEI become protonated making the formation of Au(N-(R-H))$_4^{3+}$ complexes less and less favorable, as well as the enhanced
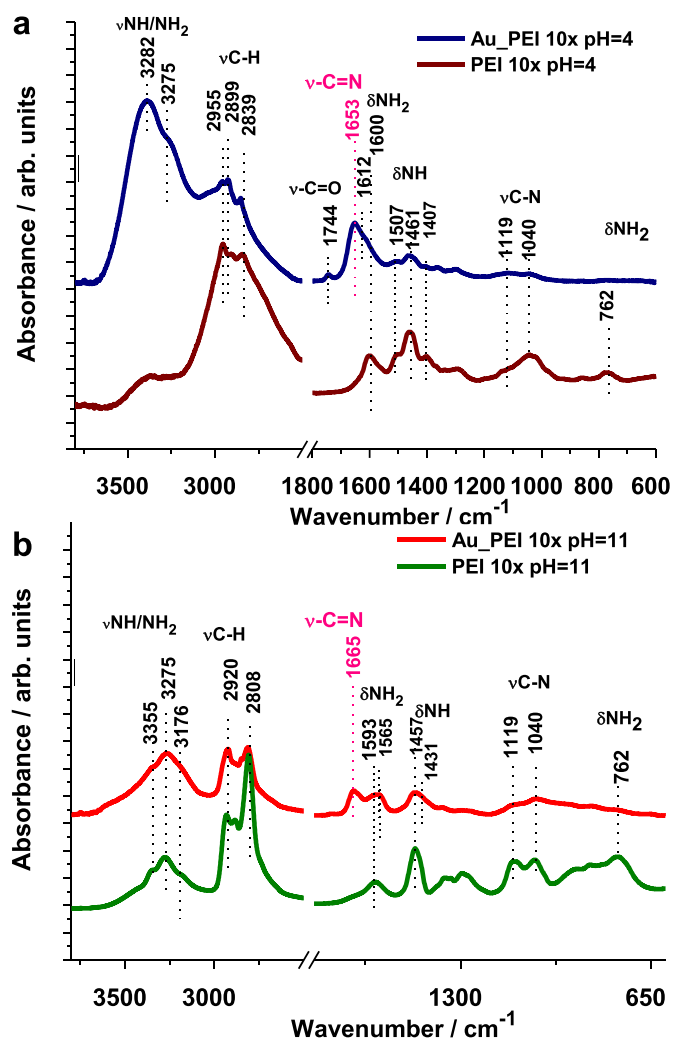
Fig. 11. Comparison of the ATR-IR spectra of Au-PEI NPs with the spectra of PEI molecules a.) at pH = 4 (the pH of the PEI solution (1 w/w%) was adjusted with HCl and the Au-PEI NPs prepared without any additives). b.) at pH = 11 (pure PEI solution (1 w/w%) without pH adjusting was used and the Au-PEI NPs were prepared in the presence of 10 mM NaOH). All mixtures were prepared at the same PEI/HAuCl$_4$ ratio, but with ten times higher absolute concentrations of the components then in the previous systems (Figs. 1–10). c_{Au} = 2 mM and c_{PEI} = 12 mM.

Fig. 12. The UV–Vis spectra of mixtures containing 0.2 mM HAuCl$_4$ and 1.2 mM PEI in the presence of other additives directly after solution preparation a.) in acidic (pH ≤ 4) and b.) in alkaline medium (pH > 11).

ionic strength leads to the coagulation of the gold nanoassemblies and precipitation during their synthesis.

In alkaline medium (i.e. at pH ≥ 10), the initial gold(III) complexes are largely different from the ones formed at low pH as shown in Fig. 12. Under these conditions, the gold(III) ions are initially present in the form of planar Au(III)(Cl$^-$)$_x$(OH$^-$)$_y$ complexes with a large excess of hydroxide ions (at pH = 10.4, for instance, x ≅ 0.1 and y ≅ 3.9) [32]. At the same time, in the highly basic pH range only a very little fraction of the primary and even less of the secondary amine groups of PEI are protonated [30]. As indicated in Fig. 12b, the addition of PEI to HAuCl$_4$ in the presence of 10 mM NaOH leads to a largely different (colorless) Au(III)/PEI complex as compared to the ones formed at low pH. These complexes are in the mixed amine-amido Au(N(R-H)$_3$(R$^-$))$^{2+}$ or amine-hydroxide Au(N(R-H)$_x$(OH$^-$)$_y$)$^{2+}$ planar form [41].

In alkaline medium, the secondary amine groups are expected to govern primarily the reduction of gold(III) ions [23,43]. However, in contrast to the acidic pH range, there is no stabilizing electrostatic repulsion between the formed gold NPs; therefore, they can aggregate/fuse into each other during the synthetic procedure. This process could either occur within a PEI molecule or between Au NPs belonging to

different polyamine molecules. Furthermore, in alkaline medium the formation of carbon radicals is enhanced from imine radical cations [40], thus, crosslinking may occur within and between the PEI molecules. This could lead to a superstructure, where gold NPs and/or agglomerates are embedded in a large network of cross-linked PEI molecules, resulting in much larger mean Stokes diameter (from DLS) of the nanoassemblies compared to the size of their primary gold NP building blocks (from TEM). Although this polymer network may be too loose to be seen in the TEM images, it provides a pronounced steric stabilization of the Au-PEI NP agglomerates. The low amount of negative charges of the gold nanoassemblies in alkaline medium is attributed to the amine carboxylate groups, which is suggested by the ATR-IR spectra.

Via the application of large electrolyte concentration, the extension of PEI molecules decreases. More importantly, the type of added electrolyte could also affect the hydration of PEI molecules. Kretschmer et al. reported recently the synthesis of a supraparticle Au-PEI nanosystems, where a large number of small gold NPs were entrapped separately in a polymer film [26]. However, these supraparticle Au-PEI assemblies were synthetized in dimethyl formamide (DMF) and then transferred into water. It is likely that the specific hydration of perchlorate ions
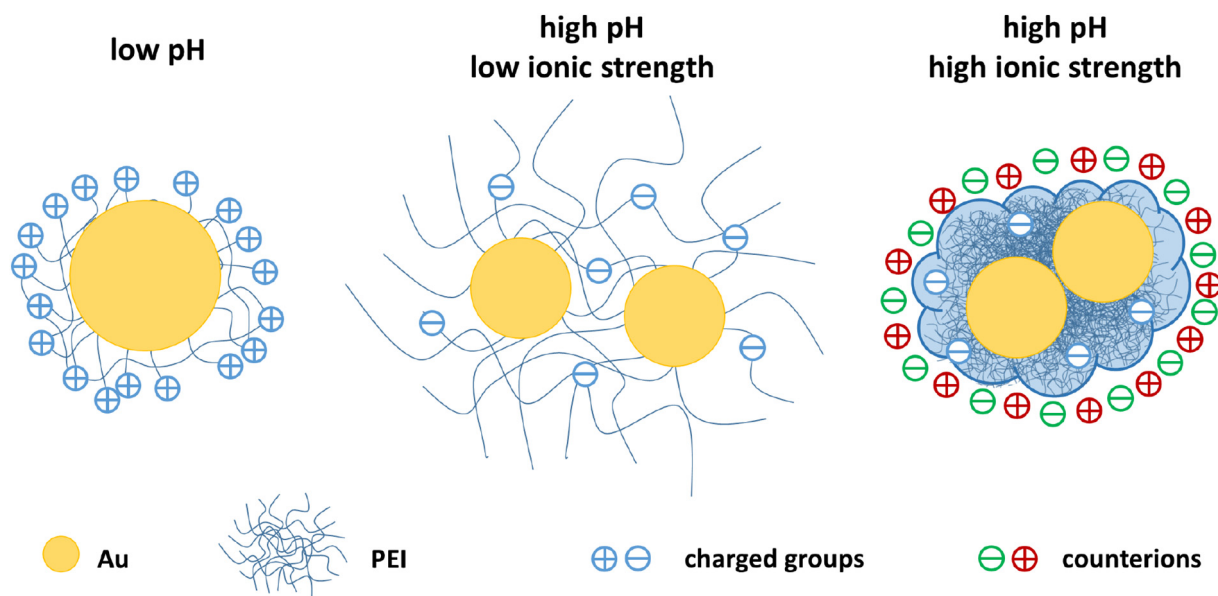
Scheme 1. Schematic illustration of the pH and NaClO$_4$ concentration dependent morphology of the Au-PEI nanoassemblies.

[34] affects the solvency of PEI molecules at high pH in such a way, which accelerates the formation of carbon radicals and thus the cross-linking processes between the ethylene imine groups (similarly as in DMF). This results in a largely cross-linked PEI film around the gold nanoparticles in alkaline medium with large NaClO$_4$ concentrations. This is also in line with the increased relative ratio of the primary amine groups in the Au-PEI nanoassemblies under these experimental conditions (as demonstrated in Fig. S8).

4. Conclusions

In the present contribution, we have shown that controlling the pH, as well as the type and concentration of added electrolytes during the synthesis, Au-PEI nanoassemblies of different morphology and charge can be prepared. The structure of these nanomaterials is far more complicated to be considered as simple PEI coated or capped gold nanoparticles as they are usually referred to.

Our major results are summarized in Scheme 1. At low pH and ionic strengths, the initial gold(III)/amine complex formation and that of the reduction processes of the Au^{3+} ions occur in the internal part of the PEI molecules due to the largely different protonation degrees of the primary, secondary and tertiary amine groups. At an optimal acidic pH and HClO$_4$ concentration, positively charged gold NPs stabilized electrosterically via a thin layer of slightly cross-linked PEI molecules can be produced. With decreasing pH or increasing electrolyte concentration, however, dispersions of larger gold NP agglomerates with reduced stability are formed.

In alkaline medium, the initial gold(III)/amine complex formation is equally possible for all of the ethyleneimine groups of PEI due to their nearly negligible protonation degree. This leads to a completely different morphology of the polymer entrapped gold nanoassemblies- compared to the ones synthetized at low pH- with low negative electrokinetic charge density. At low NaClO$_4$ concentrations, gold NP agglomerates embedded in a loosely cross-linked network of several PEI molecules are formed, which provides significant steric stabilization. With increasing ionic strength, the extension of this polymer matrix may decrease, however the stability of the gold nanosystems does not reduce. The simultaneous application of large concentrations of sodium perchlorate and NaOH considerably changes the mechanism of oxidative dehydrogenation of the amine groups as well as accelerate the subsequent fusion and cross-linking processes as compared to

other types of salt and/or the acidic medium. This leads to gold NPs embedded in a coherent amorphous film of largely cross-linked PEI molecules, which could provide a significant steric hindrance against aggregation.

The present study indicates that stable gold NPs entrapped in a polymer matrix with very different charge, morphology, extension and elasticity can be synthetized by careful variation of the pH and electrolyte additives. These results may be further exploited in novel applications of Au-PEI nanoassemblies.

CRediT authorship contribution statement

Krisztina Bali: Conceptualization, Methodology, Writing - original draft. **Mónika Bak:** Investigation, Data curation. **Katarina Szarka:** Investigation, Visualization. **György Juhász:** Validation, Data curation. **György Sáfrán:** Formal analysis. **Béla Pécz:** Formal analysis, Writing - review & editing. **Judith Mihály:** Validation, Methodology. **Róbert Mészáros:** Conceptualization, Methodology, Supervision, Writing - review & editing.

Declaration of competing interest

The authors declare that they have no known competing financial interests or personal relationships that could have appeared to influence the work reported in this paper.

Appendix A. Supplementary data

https://www.journals.elsevier.com/journal-of-molecular-liquids Supplementary data to this article can be found online at https://doi.org/10.1016/j.molliq.2020.114559.

References

[1] M.-C. Daniel, D. Astruc, Gold nanoparticles: assembly, supramolecular chemistry, quantum-size-related properties, and applications toward biology, catalysis, and nanotechnology, Chem. Rev. 104 (2004) 293–346.

[2] M. Sharifi, F. Attar, A.A. Saboury, K. Keivan Akhtari, N. Nasrin Hooshmand, A. Hasan, M.A. El-Sayed, M. Falahati, Plasmonic gold nanoparticles: optical manipulation, imaging, drug delivery and therapy, J. Control. Release 311–312 (2019) 170–189.

[3] B. Peter, I. Lagzi, S. Teraji, I. Nakanishi, L. Cervenak, D. Zámbó, A. Deák, K. Molnár, M. Truszka, I. Szekacs, R. Horvath, Interaction of positively charged gold nanoparticles with cancer cells monitored by an in situ label-free optical biosensor and transmission electron microscopy, ACS Appl. Mater. Interfaces 10 (2018) 26841–26850.

[4] T. Ishida, T. Murayama, A. Taketoshi, M. Haruta, Importance of size and contact structure of gold nanoparticles for the genesis of unique catalytic processes, Chem. Rev. 120 (2020) 464–525.

[5] O. Boussif, F. Lezoualch, M.A. Zanta, M.D. Mergny, D. Scherman, B. Demeneix, J.P. Behr, A versatile vector for gene and oligonucleotide transfer into cells in culture and in-vivo -polyethylenimine, Proc. Natl. Acad. Sci. U. S. A. 92 (1995) 7297–7301.

[6] K. Tonigold, I. Varga, T. Nylander, R.A. Campbell, Effects of aggregates on mixed adsorption layers of poly(ethylene imine) and sodium dodecyl sulfate at the air/liquid interface, Langmuir 25 (2009) 4036–4046.

[7] K. Pojják, R. Mészáros, Preparation of stable electroneutral nanoparticles of sodium dodecyl sulfate and branched poly(ethylenimine) in the presence of Pluronic F108 copolymer, Langmuir 27 (2011) 14797–14806.

[8] A.K. Sharma, S. Shankhwar, M.S. Gaur, PEI-conjugated AuNPs as a sensing platform for arsenic (AS-III), J. Exp. Nanosci. 9 (2014) 892–905.

[9] K.M. Kim, Y.-S. Nam, Y. Lee, K.-B. Lee, A highly sensitive and selective colorimetric Hg^{2+} ion probe using gold nanoparticles functionalized with polyethyleneimine, J. Anal. Methods Chem. 2018 (2018), 1206913, 12 pages.

[10] S. Wen, F. Zheng, M. Shen, X. Shi, Synthesis of polyethylenimine-stabilized gold nanoparticles for colorimetric sensing of heparin, Colloids Surf. A Physicochem. Eng. Asp. 419 (2013) 80–86.

[11] M. Thomas, A.M. Klibanov, Conjugation to gold nanoparticles enhances polyethylenimine's transfer of plasmid DNA into mammalian cells, Proc. Natl. Acad. Sci. U. S. A. 100 (2003) 9138–9143.

[12] Y. Zhang, S. Wen, L. Zhao, D. Li, C. Liu, W. Jiang, X. Gao, W. Gu, N. Ma, J. Zhao, X. Xiangyang Shi, Q. Zhao, Ultrastable polyethylenimine-stabilized gold nanoparticles modified with polyethylene glycol for blood pool, lymph node and tumor CT imaging, Nanoscale 8 (2016) 5567–5577.

[13] G.G. Lazarus, M. Singh, In vitro cytotoxic activity and transfection efficiency of polyethyleneimine functionalized gold nanoparticles, Colloids Surf., B 145 (2016) 906–911.

[14] Z. Benqing, Z. Xiong, P. Wang, C. Peng, M. Shen, X. Shi, Acetylated polyethylenimine-entrapped gold nanoparticles enable negative computed tomography imaging of orthotopic hepatic carcinoma, Langmuir 34 (2018) 8701–8707.

[15] T.J. Cho, J.M. Gorham, J.M. Pettibone, J. Liu, J. Tan, V.A. Hackley, Parallel multi-parameter study of PEI-functionalized gold nanoparticle synthesis for bio-medical applications: part 1—a critical assessment of methodology, properties, and stability, J. Nanopart. Res. 21 (2019) 188.

[16] V. Mulens-Arias, A. Nicolás-Boluda, A. Gehanno, A. Balfourier, F. Carn, F. Gazeau, Polyethyleneimine-assisted one-pot synthesis of quasi-fractal plasmonic gold nanocomposites as a photothermal theranostic agent, Nanoscale 11 (2019) 3344–3359.

[17] A. Philip, B. Ankudze, T.T. Pakkanen, Polyethylenimine-assisted seed-mediated synthesis of gold nanoparticles for surface-enhanced Raman scattering studies, Appl. Surf. Sci. 444 (2018) 243–252.

[18] I.-H. Kim, J. Hoon Kim, J.-Y. Choi, J. Ho Shin, J.-H. Kim, G.-T. Bae, K. Soo Shin, Tuning the interparticle distances in self-assembled gold nanoparticle films with their plasmonic responses, Chem. Phys. Lett. 715 (2019) 91–99.

[19] T.J. Cho, J.M. Pettibone, J.M. Gorham, T.M. Nguyen, R.I. MacCuspie, J. Gigault, V.A. Hackley, Unexpected changes in functionality and surface coverage for au nanoparticle PEI conjugates: implications for stability and efficacy in biological systems, Langmuir 31 (2015) 7673–7683.

[20] X. Sun, S. Dong, E. Wang, One-step synthesis and characterization of polyelectrolyte-protected gold nanoparticles through a thermal process, Polymer 45 (2004) 2181–2184.

[21] X. Sun, S. Dong, E. Wang, One-step preparation of highly concentrated well-stable gold colloids by direct mix of polyelectrolyte and $HAuCl_4$ aqueous solutions at room temperature, J. Colloid Interface Sci. 288 (2005) 301–303.

[22] S.T. Wang, J.C. Yan, L. Chen, Formation of gold nanoparticles and self-assembly into dimer and trimer aggregates, Mater. Lett. 59 (2005) 1383–1386.

[23] X. Sun, S. Dong, E. Wang, One-step polyelectrolyte-based route to well-dispersed gold nanoparticles: synthesis and insight, Mater. Chem. Phys. 96 (2006) 29–33.

[24] R. Kim, H.S. Park, T. Yu, J. Yi, W.-S. Woo-Sik Kim, Aqueous synthesis and stabilization of highly concentrated gold nanoparticles using sterically hindered functional polymer, Chem. Phys. Lett. 575 (2013) 71–75.

[25] T. Yu, R. Kim, H. Park, J. Yi, W.-S. Kim, Mechanistic study of synthesis of gold nanoparticles using multi-functional polymer, Chem. Phys. Lett. 592 (2014) 265–271.

[26] F. Kretschmer, U. Mansfeld, S. Hoeppener, M.D. Hager, U.S. Schubert, Tunable synthesis of poly(ethylene imine)–gold nanoparticle clusters, Chem. Commun. 50 (2014) 88–90.

[27] N.P.B. Tan, C.H. Lee, L. Chen, K.M. Ho, Y. Lu, M. Ballauff, P. Li, Facile synthesis of gold/polymer nanocomposite particles using polymeric amine-based particles as dual reductants and templates, Polymer 76 (2015) 271–279.

[28] K. Bali, G. Sáfrán, B. Pécz, R. Mészáros, Preparation of gold nanocomposites with tunable charge and hydrophobicity via the application of polymer/surfactant complexation, ACS Omega 2 (2017) 8709–8716.

[29] K. Bali, B. Dúzs, G. Sáfrán, B. Pécz, R. Mészáros, Effect of added surfactant on poly (ethylenimine)-assisted gold nanoparticle formation, Langmuir 35 (2019) 14007–14016.

[30] G.J.M. Koper, M. Borkovec, Proton binding by linear, branched, and hyperbranched polyelectrolytes, Polymer 51 (2010) 5649–5662.

[31] D.C. Henry, The cataphoresis of suspended particles. Part I.—the equation of cataphoresis, Proc. Roy. Soc. A133 (1931) 106–129.

[32] S. Wang, K. Qian, X. Bi, W. Huang, Influence of speciation of aqueous $HAuCl_4$ on the synthesis, structure, and property of au colloids, J. Phys. Chem. C 113 (2009) 6505–6510.

[33] R. Mészáros, L. Thompson, M. Bos, P. de Groot, Adsorption and electrokinetic properties of polyethylenimine on silica surfaces, Langmuir 18 (2002) 6164–6169.

[34] H. Hofmeister, Fivefold twinned nanoparticles, in: H.S. Nalwa (Ed.), Encyclopedia of Nanoscience and Nanotechnology, vol. 3, American Scientific Publisher 2004, pp. 431–452.

[35] G. Socrates, Infrared and Raman Characteristic Group Frequencies: Tables and Charts, 3. Ed., Repr. As Paperback, Wiley, Chichester, 2010.

[36] F. Wang, P. Liu, T. Nie, H. Wei, Z. Cui, Characterization of a polyamine microsphere and its adsorption for protein, Int. J. Mol. Sci. 14 (2012) 17–29.

[37] F. Long, Z. Chen, K. Han, L. Zhang, W. Zhuang, Differentiation between enamines and tautomerizable imines oxidation reaction mechanism using electron-vibration-vibration two dimensional infrared spectroscopy, Molecules 24 (2019) 869.

[38] Y. Chen, Y.-H. Zhang, L.-J. Zhao, ATR-FTIR spectroscopic studies on aqueous $LiClO_4$, $NaClO_4$, and $Mg(ClO_4)_2$ solutions, PCCP 6 (2004) 537–542.

[39] F.R. Keene, Metal-ion promotion of the oxidative dehydrogenation of coordinated amines and alcohols, Coord. Chem. Rev. 187 (1999) 121–149.

[40] J. Hu, J. Wang, T.H. Nguyen, N. Zheng, The chemistry of amine radical cations produced by visible light photoredox catalysis, Beilstein J. Org. Chem. 9 (2013) 1977–2001.

[41] A.K. Gangopadhayay, A. Chakravorty, Charge transfer spectra of some gold(III) complexes, J. Chem. Phys. 35 (1961) 2206–2209.

[42] P.-L. Kuo, C.-C. Chen, Generation of gold thread from Au(III) and triethylamine, Langmuir 22 (2006) 7902–7906.

[43] A. Köth, J. Koetz, D. Appelhans, B. Voit, "Sweet" gold nanoparticles with oligosaccharide-modified poly(ethyleneimine), Colloid Polym. Sci. 286 (2008) 1317–1327.